Acta Geologica Sinica (English Edition), 2019, 93(supp.1): 173–176

A Modified Transformed Soil Adjusted Vegetation Index for Cropland in Jilin Province, China

ZHEN Zhijun, CHEN Shengbo*, QIN Wenhan, LI Jian, Murefu MIKE and YANG Beiping

College of Geo-Exploration Science and Technology, Jilin University, Changchun 130026, China

Citation: Zhen et al., 2019. A Modified Transformed Soil Adjusted Vegetation Index for Cropland in Jilin Province, China. *Acta Geologica Sinica* (English Edition), 93(supp. 1): 173-176

1 Introduction

Vegetation indices (VIs) derived from satellite observations are an essential source of information for operational monitoring of the Earth's vegetation (Qu et al., 2018; Yan et al., 2008). However, soil background dramatically affects the performances of VIs (Baret and Guyot, 1991; Gilabert et al., 2002; Huete, 1988; Qi et al., 1994). So soil-adjusted VIs (Baret and Guyot, 1991; Gilabert et al., 2002; Huete, 1988; Qi et al., 1994) are designed in order to minimize the soil noise. However, these commonly used vegetation indices requires prior knowledge: the so-called soil-adjustment factor.

Soil-adjustment factor is related to canopy structure parameters and the choice of the value of soil-adjustment factor appears to be quite critical in minimizing soil background noise (Huete, 1988; Qi et al., 1994). In order to replace the constant soil adjustment factor that require prior knowledge, MSAVI is proposed by developing an iterative function of soil adjustment factor (Qi et al., 1994). However, the inductive function is only based on one the assumption that soil adjustment factor can only vary between 0 and 1. Recently studies have shown that negative soil adjustment factor performs better in arid grasslands areas (Ren et al., 2018). Thus, it is important to build an appropriate iterative function.

Iterative function describes the relationship between the value of VIs and soil adjustment factor. Therefore, the key to establish the iterative function is to estimate the optimal soil adjustment factor under different vegetation conditions. SAVI-family VIs assume that all the vegetation isolines converge to one common point, and the location of that point is soil adjustment factor (Baret and Guyot, 1991; Gilabert et al., 2002; Huete, 1988; Qi et al., 1994). However, in real vegetation isolines do not coverage to one point, they all intersected with soil line at different points (Ren et al., 2018). Among all the SAVI-family VIs, only TSAVI take into consideration of soil line. By investigating the cross point between vegetation isolines and soil line, it is capable to find the optimal soil adjustment factor. Thus it is feasible to estimate the optimal soil adjustment factor of TSAVI. However, little attention has been payed to build a self-adjustable *X* function for TSAVI.

In this study, a self-adjusted function of soil adjusted factor is designed to replace the constant soil adjusted factor ($X = 0.08$) in TSAVI by using mathematic induction method. It will improve the TSAVI vegetation sensitivity by increasing the dynamic range and further reducing the soil background influence. The result would be an improved, Modified TSAVI (MTSAVI) with better performance in agricultural crops or homogeneous plant canopies with high vegetation cover.

* Corresponding author. E-mail: chensb@jlu.edu.cn

2 Materials and methods

2.1 An inductive *X* function

Most VIs relies on a major simplifying hypothesis on the vegetation islolines: these lines are parallel or convergent at one common point (Baret et al., 1989; Huete, 1988; Qi et al., 1994). However, in real they intersected with soil line at different locations (Ren et al., 2018). By assigning negative abscissa of interested point to corresponding *X* of TSAVI, the TSAVI isolines are almost the same as true vegetation isolines. However, it is extremely difficult to find every crossing point between each isolines and soil line without prior knowledge.

One potential solution to this problem is to use inductive method to build a self-adjusted *X* (Qi et al., 1994). To distinguish this new vegetation index from TSAVI (X=0.08), we call this new index Modified TSAVI (MTSAVI). By defining an

$$X = c - d \cdot \mathrm{MTSAVI} \tag{1}$$

inductive *X* function as

where *c* and *d* are parameters of inductive *X* function. Then

$$\mathrm{MTSAVI} = \frac{\left[a \cdot nir + red - a \cdot b + c \cdot \left(1 + a^2\right)\right]}{2d \cdot \left(1 + a^2\right)} - \frac{\sqrt{\left[a \cdot nir + red - a \cdot b + c \cdot \left(1 + a^2\right)\right]^2 - 4d \cdot \left(1 + a^2\right) \cdot a \cdot \left(nir - a \cdot red - b\right)}}{2d \cdot \left(1 + a^2\right)} \tag{2}$$

the MTSAVI based on TSAVI can be written as:

where *red* and *nir* are the reflectance in the red and near-infrared band, *a* and *b* are the parameters of the soil line. Thus it is crucial to find the parameters *c* and *d* in the relationship between *X* and MTSAVI.

2.2 Data

Simulated data is used to fit the inductive *X* function. Simulation modelling of canopy bidirectional reflectances factor is applied to obtain different scenes with varying canopy structure factors Leaf Area Index (LAI) and Average leaf angle (ALA) as well as soil optical property (Baret and Guyot, 1991) by using Discrete Anisotropic Radiative Transfer (DART) model (Gastellu-Etchegorry and Bruniquel-Pinel, 2001; Gastellu-Etchegorry et al., 2017; Gastelluetchegorry et al., 1996; Yin et

http://www.geojournals.cn/dzxbcn/ch/index.aspx
https://onlinelibrary.wiley.com/journal/17556724

al., 2017; Yin et al., 2016) (http://www.cesbio.ups-tlse.fr/dart).

To verify the robustness of MTSAVI, high-resolution reflectance data sets from one laboratory experiments is used (Garcã. A-Haro et al., 1996). A set of 21 plots was designed, consisting of seven varying amounts of vegetation (Quercus ilex rotundifolia) over three different soil backgrounds. LAI was measured using a LICOR-2000 LAI canopy analyzer, and reflectance data were obtained for each plot using a GER SIRIS spectroradiometer.

3 Results and discussions

3.1 Relationship between foliage cover and soil adjustment factor

The foliage cover is calculated using LAI and ALA (Campbell, 1986; Rondeaux et al., 1996). The scatter graph between foliage coverage and optimal X was plotted (Fig. 1). Vegetation isolines tend to be parallel to each other and the abscissa of the intersection point with soil line is low (the optimum value of X is high) when the foliage coverage is low. However, when the foliage coverage is high, the vegetation contour tends to intersect at one point on the soil line, and the abscissa of the intersecting point is high (the optimum value of X is low) (Fig. 1). This is ignored by previous researchers and may explain why PVI which assuming that vegetation isolines are parallel to each other performs better in low coverage area whereas SAVI which assuming that vegetation isolines converge to one common point performs better in high coverage area.

Our result agrees on the conclusion that the soil-adjustment factor became lower in value as vegetation became denser (Gilabert et al., 2002; Huete, 1988; Qi et al., 1994). Besides, the value of soil-adjustment factor is the negative value of abscissa crossing point, so our result also conforms with the conclusion that high vegetation isolines tended to intersect with soil line further away from the origin, while low vegetation isolines tended to converge close to the origin (Ren et al., 2018), even though Ren et al. (2018) claim that his conclusion counter to Gilabert et al. (2002), Huete (1988) and Qi et al. (1994). The reason why Ren et al. (2018)' s conclusion is contrary is that he uses the absolute distance from origin to the cross-point to describe the optimal soil-adjustment factor rather than coordinates. So when the value of optimal soil-adjustment factor changes from positive to negative, absolute distance of cross-point from origin is increasing, but the abscissa value of crossing point is still decreasing.

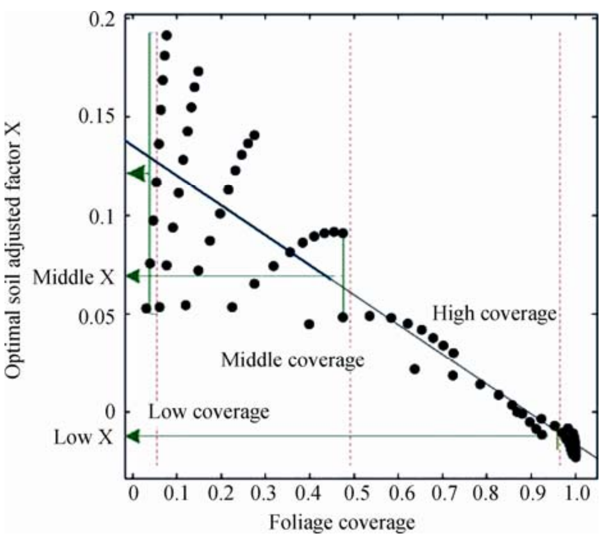

Fig. 1. The relationship between optimal X and foliage coverage using simulated data.

3.2 Relationship between optimal *X*, LAI and ALA

To evaluate the influence of LAI and ALA on optimal X, the scatter graph between optimal X and TSAVI calculated using the optimal X values was plotted (Fig. 2). Scatter distribution is almost the same as foliage coverage. LAI always influence the optimal X dramatically, while ALA only dramatically influence X when LAI is low. Besides, when LAI is less than 1, optimal X is negatively correlated with ALA. However, when LAI is over 1, X value is positively correlated with ALA. Besides, the value of soil adjusted factor decrease and converge to one point as TSAVI rise. All these are ignored by previous researchers.

3.3 Discussion

Considering foliage coverage is less than 0.5 or LAI is less than 1.6, vegetation contour lines are approximately parallel to each other and intersect with soil contour lines at different points, which is more consistent with the assumption of PVI, and it is difficult to determine the value of the optimal soil-adjustment factor. Thus MTSAVI may not be a good choice in sparsely vegetated area. However, when foliage coverage is greater than 0.5 or LAI is greater than 1.6, vegetation isolines tend to intersect with soil lines at one common point on the soil line, which is more consistent with the assumption of soil regulated vegetation index and easier to determine the value of the optimal soil-adjustment factor.

In this paper, simulated data with foliage coverage greater than 0.5 is used to fit the two coefficients c and d in the equation (1) as 0.2 and 0.1 respectively, and the laboratory data is used for verification. Considering SAVI family VIs may not be a good choice in sparsely vegetated area, MTSAVI is designed only for agricultural crops or homogeneous plant canopies with high vegetation cover. Thus only LAI being over 1.3 in laboratory

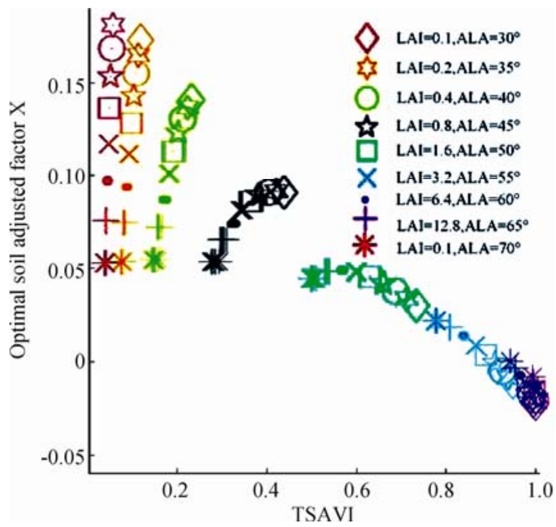

Fig. 2. The relationship between soil-adjustment factor X, LAI and ALA.

Different color represents different LAI while different symbols represents different ALA. TSAVI is calculated using the optimal soil adjusted factor X rather than constant X=0.08.

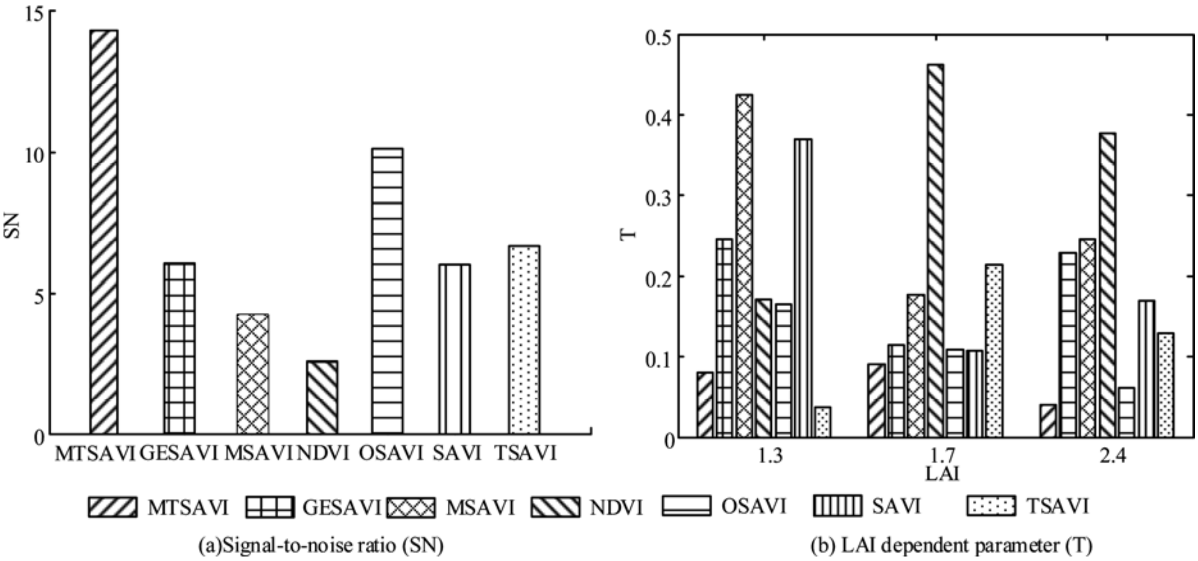

Fig. 3. Performances of vegetation for (a) Signal-to-noise ratio (SN) and (b) LAI dependent parameter (T).
The higher SN and the lower T means the better performance of VIs.

data are used in this study to verify the performance of MTSAVI. Two evaluation criterion are used including signal-to-noise ratio (S/N) (Leroy and Roujean, 1994) and LAI dependent parameter (T) (Gilabert et al., 1998).

$$\frac{S(VI)}{N(VI)} = \frac{\overline{VI(LAI_{max})} - \overline{VI(LAI_{min})}}{\int_{LAI_{min}}^{LAI_{max}} \left[\max VI(LAI) - \min VI(LAI)\right] d(LAI)} \tag{3}$$

Signal-to-noise ratio (S/N) is defined as:

$$T_{VI}(LAI) = \frac{\sigma_{LAI}}{\bar{\sigma}} \times 100 \tag{4}$$

LAI dependent parameter (T) is defined as:

where σ_{LAI} is the standard deviation of the VI value according to the value of LAI assigned, $\bar{\sigma}$ is the standard deviation of the entire VI value considering the range of LAI variation. MTSAVI yield better performance both for S/N and T (Fig. 3). MTSAVI is used to monitoring Cropland in Jiutai and Dehui City, Changchun province, China (Fig. 4).

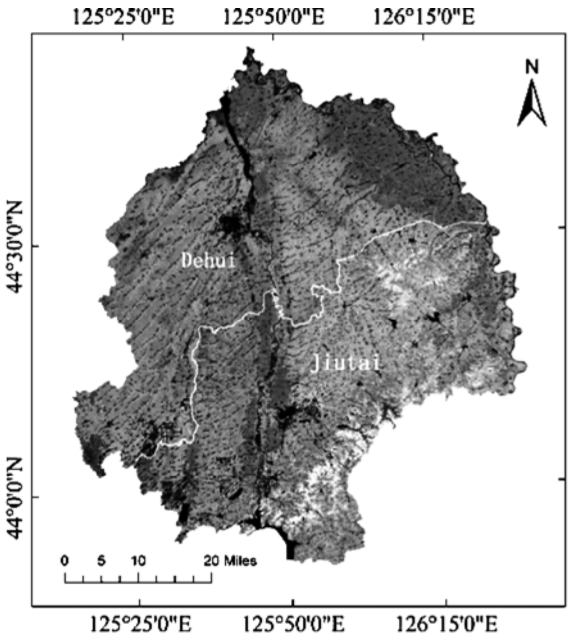

Fig. 4. Cropland monitoring based on MTSAVI in Jiutai and Dehui City, Changchun Province, China.

4 Conclusion

The purpose of this paper is to developed a self-adjustable X that do not require prior knowledge to replace the constant $X = 0.08$ in the TSAVI equation. It can further reduce the soil background effect by increasing the dynamic range, so as to improve the sensitivity of TSAVI to vegetation. Two data sets including simulated and laboratory data are used in this study. Simulated data show that vegetation isolines tend to be parallel to each other and the abscissa of the intersection point with soil line is low when the foliage coverage is low. However, when the foliage coverage is high, the vegetation contour tends to intersect at one point on the soil line, and the abscissa of the intersecting point is high. Besides, LAI always influence the optimal X dramatically, while ALA only dramatically influence X when LAI is low. When LAI is less than 1, optimal X is negatively correlated with ALA. However, when LAI is over 1, X value is positively correlated with ALA. Laboratory data are used to validly the robustness of MTSAVI in high foliage coverage area. Current research has shown this potential, but more thorough verifications are also needed. A further study concerning investigation on temporal dynamic response to cropland in Changchun, China.

Key words: remote sensing, vegetation indices, soil-adjustment factor, induction function

Acknowledgments: This work is granted by Land Resources Evolution Mechanism and Sustainable Use in Global Black Soil Critical Zone (IGCP 665) and Geochemical Survey of Land Quality in 1:25 Northeast China Black Soil (Grant No. DD20160316).

References

Baret, F., and G. Guyot, 1991. Potentials and limits of vegetation indices for LAI and APAR assessment. *Remote Sensing of Environment*, 35: 161–173.

Baret, F., G. Guyot, and D.J. Major, 1989. TSAVI: A Vegetation Index Which Minimizes Soil Brightness Effects On LAI And APAR Estimation. *Geoscience and Remote Sensing Symposium 1989. Canadian Symposium on Remote Sensing* 1989: 1355–1358.

Campbell, G. S., 1986. Extinction coefficients for radiation in plant canopies calculated using an ellipsoidal inclination angle distribution. *Agricultural & Forest Meteorology*, 36: 317–321.

Garcã A-Haro, F. J., M.A. Gilabert, and J. Meliã, 1996. Linear spectral mixture modelling to estimate vegetation amount from optical spectral data. *International Journal of Remote Sensing*, 17: 3373–3400.

Gastellu-Etchegorry, J.P., and V. Bruniquel-Pinel, 2001. A modeling approach to assess the robustness of spectrometric predictive equations for canopy chemistry. *Remote Sensing of Environment*, 76: 1–15.

Gastellu-Etchegorry, J.P., N. Lauret, T. Yin, L. Landier, and Z. Mitraka, 2017. DART: Recent Advances in Remote Sensing Data Modeling With Atmosphere, Polarization, and Chlorophyll Fluorescence. *IEEE Journal of Selected Topics in Applied Earth Observations & Remote Sensing*, PP: 1–10.

Gastelluetchegorry, J.P., F. Zagolski, and J. Romier, 1996. A simple anisotropic reflectance model for homogeneous multilayer canopies. *Remote Sensing of Environment*, 57: 22–38.

Gilabert, M.A., J. González-Piqueras, F. J. GarcíA-Haro, and J. Meliá, 2002. A generalized soil-adjusted vegetation index. *Remote Sensing of Environment*, 82: 303–310.

Gilabert, M.A., J.G. Piqueras, J. Garciaharo, and J. Melia, 1998. Designing a generalized soil-adjusted vegetation index (GESAVI). *Remote Sensing*, 3499: 396–404.

Huete, A. R., 1988. A soil-adjusted vegetation index (SAVI). *Remote Sensing of Environment*, 25: 295–309.

Leroy, M., and J. Roujean, 1994. Sun and view angle corrections on reflectances derived from NOAA/AVHRR data. *IEEE Transactions on Geoscience and Remote Sensing*, 32: 684–697.

Qi J., A. Chehbouni, A.R. Huete, Y. H. Kerr, and S. Sorooshian, 1994. A modified soil adjusted vegetation index. *Remote Sens Envrion*, 48: 119–126.

Qu Y., A. Shaker, C. Silva, C. Klauberg, and E. Pinagé, 2018. Remote Sensing of Leaf Area Index from LiDAR Height Percentile Metrics and Comparison with MODIS Product in a Selectively Logged Tropical Forest Area in Eastern Amazonia. *Remote Sensing*, 10: 970 –993.

Ren H., G. Zhou, and F. Zhang, 2018. Using negative soil adjustment factor in soil-adjusted vegetation index (SAVI) for aboveground living biomass estimation in arid grasslands. *Remote Sensing of Environment*, 209: 439–445.

Rondeaux, G., M. Steven, and F. Baret, 1996. Optimization of soil-adjusted vegetation indices. *Remote Sensing of Environment*, 55: 95–107.

Yan G., X. Mu, Y. Ma, and Z. L. Li, 2008. A strategy to integrate a priori knowledge for an improved inversion of the LAI from BRDF modelling. *International Journal of Remote Sensing*, 29: 4927–4941.

Yin T., S. Kotthaus, J.-P. Gastellu-Etchegorry, W. Morrison, L. Norford, C. Grimmond, N. Lauret, N. Chrysoulakis, A. Al Bitar, and L. Landier, 2017. Atmospheric correction of ground -based thermal infrared camera through dart model. *2017 IEEE International Geoscience and Remote Sensing Symposium*, 5885–5888.

Yin T., N. Lauret, and J.P. Gastellu-Etchegorry, 2016. Simulation of satellite, airborne and terrestrial LiDAR with DART (II): ALS and TLS multi-pulse acquisitions, photon counting, and solar noise. *Remote Sensing of Environment*, 184: 454–468.

About the first author

ZHEN Zhijun, male, born in 1994 in Baiyin City, Gansu Province; BS; graduated from Jilin University; Ph.D. student in Jilin University. He is now interested in the study on quantitative remote sensing. Email: zhenzj18@mails.jlu.edu.cn; phone: 18844193741.

About the corresponding author

CHEN Shengbo, male, born in 1967 in Luoshan City, Henan Province; PhD; graduated from institute of geographic sciences and natural resources research; professor of College of Geoexploration science and technology, Jilin University. He is now interested in the study on quantitative remote sensing. Email: chensb@jlu.edu.cn; phone: 13689805788.